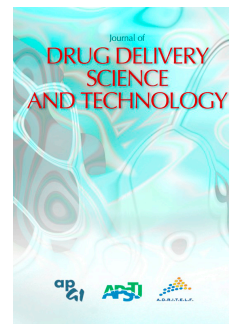# Accepted Manuscript

Dual stimuli-responsive polypyrrole nanoparticles for anticancer therapy

Rania M. Hathout, AbdelKader A. Metwally, Sherweit H. El-Ahmady, Eman S. Metwally, Noha A. Ghonim, Salma A. Bayoumy, Tarek Erfan, Rosaline Ashraf, Maha Fadel, Abdullah I. El-Kholy, John G. Hardy

Please cite this article as: R.M. Hathout, A.A. Metwally, S.H. El-Ahmady, E.S. Metwally, N.A. Ghonim, S.A. Bayoumy, T. Erfan, R. Ashraf, M. Fadel, A.I. El-Kholy, J.G. Hardy, Dual stimuli-responsive polypyrrole nanoparticles for anticancer therapy, *Journal of Drug Delivery Science and Technology* (2018), doi: 10.1016/j.jddst.2018.07.002.

Electricity

Polypyrrole nanoparticles

Light

Electrochemically-triggered release of an anticancer drug

Photothermally-triggered anticancer effect

NIR Laser

Cancer Cell Ablation

Dual stimuli-responsive polypyrrole nanoparticles for anticancer therapy

Rania M. Hathout[1], AbdelKader A. Metwally[1], Sherweit H. El-Ahmady[2], Eman S. Metwally[3], Noha A. Ghonim[3], Salma A. Bayoumy[3], Tarek Erfan[3], Rosaline Ashraf[3], Maha Fadel[4], Abdullah I. El-Kholy[4] and John G. Hardy[5,6]

[1] Department of Pharmaceutics and Industrial Pharmacy, Faculty of Pharmacy, Ain Shams University, African Union Street Authority Street, Abbassia, 11566, Cairo, Egypt.

[2] Department of Pharmacognosy, Faculty of Pharmacy, Ain Shams University, African Union Street Authority Street, Abbassia, 11566, Cairo, Egypt.

[3] Drug Design Program, Faculty of Pharmacy, Ain Shams University, African Union Street Authority Street, Abbassia, 11566, Cairo, Egypt.

[4] Department of Medical Applications of Laser, National Institute of Laser Enhanced Sciences, Cairo University.

[5] Department of Chemistry, Lancaster University, Lancaster, Lancashire, LA1 4YB, United Kingdom.

[6] Materials Science Institute, Lancaster University, Lancaster, Lancashire, LA1 4YB, United Kingdom.

Correspondence:

Email: j.g.hardy@lancaster.ac.uk

Telephone: +441524595080

Abstract:

We report the development of dual stimuli-responsive nanoparticles with potential for anticancer therapy. The nanoparticles are composed of a conjugated polymer (polypyrrole, PPY) loaded with an anticancer drug (allicin), and were characterized by a variety of

physicochemical techniques. The dual stimuli-responsive nature of the PPY nanoparticles was validated *in vitro*: the PPY nanoparticles delivered an anticancer drug (allicin) in response to exposure to an electric field *in vitro* as demonstrated with UV-vis spectroscopy; and the PPY nanoparticles exhibited photothermal activity upon irradiation with near infrared light which resulted in resulted in toxicity towards HEP G2 cells *in vitro*. We believe that such nanoparticles have long term potential for application in cancer therapy in a variety of tissue niches (e.g. breast cancer, liver cancer, lung cancer, skin cancer).

Keywords: polypyrrole; nanoparticles; cancer; conjugated polymer; photothermal; stimuli-responsive

1. Introduction

The global market for drug delivery systems is driven by an increasing demand for such technologies in both developed and emerging economies. The development of systems capable of controllably delivering drugs at rates determined by specific features of the systems, particularly those that respond to chemical stimuli (e.g. enzymes, ions, pH) or physical stimuli (e.g. electromagnetic fields, temperature) is an exciting avenue of research and development (Tibbit et al., 2015). A multitude of drug delivery systems that function via a single mechanism have been reported, and the development of drug delivery systems that function via multiple mechanisms (either via the delivery of a combination of therapeutics or in response to multiple stimuli) is an area of increasing investment in research and development.

Conjugated polymers have interesting optoelectronic properties which has garnered significant industrial interest for their use in technical applications (particularly in the ubiquitous electronics industry) and medical applications (e.g. for use as bioactuators, biosensors, drug delivery devices, neural electrode coatings, or indeed tissue scaffolds for tissue engineering). The conjugated polymer derivatives that are most commonly investigated

for biomedical applications are polyaniline, polypyrrole (PPY, **Figure 1A**) and polythiophene; and polyaniline- and PPY-based systems have been shown to deliver drugs with various structures (including anions and cations) in response to electrochemical triggers as described in excellent reviews (Pillay et al., 2014; Uppalapati et al., 2016). Furthermore, conjugated polymers have also been used to deliver drugs (e.g. the topoisomerase inhibitor Camptothecin) in response to near infrared (NIR) light (Wang et al., 2015).

Cancer is one of the leading causes of death worldwide and its effective treatment is therefore the focus of research supported by charities, governments and industry (Abozeid et al., 2016). While traditional anticancer drug delivery systems can be effective in certain circumstances, the use of novel drug delivery systems that maximize the therapeutic efficacy of the drugs delivered, and potentially overcome resistance mechanisms and any associated side-effects of the therapeutics to be delivered is particularly appealing (Song et al., 2017). In this context, the conjugated PPY possesses good *in-vitro* and *in-vivo* biocompatibility, which responds to exposure to irradiation with NIR light, and electrochemical stimuli, offering potential for drug delivery in response to either light or electricity, and may eventually prove to be a useful component in multi-stimuli-responsive drug delivery devices used in *in vivo* cancer therapy (Wang et al., 2017; Chen et al. 2017). NIR penetrates biological tissues deeply (typically to depths of multiple cm), with minimal/no harm to the tissues (Wang et al., 2015).

PPY can be synthesized in large quantities at room temperature in a wide range of aqueous or non-aqueous solvents either by solution phase or electrochemical polymerization. Electrochemical polymerization is appealing because it is cheap, reliable and green (Fonner et al., 2008; Balint et al., 2014); moreover, it is easy to load the polymer with a negatively charged drug (dopant) during the electrochemical polymerization. Hundreds of different anticancer drugs exist of both natural and synthetic origins (Borden et al. 1999; Curt et al.,

1996). Allicin (diallyl thiosulfinate) is a bioactive component derived from garlic (*Allium sativum*) and ramsons (*Allium ursinum*) and has been reported to show a spectrum of therapeutic effects including antimicrobial, antifungal, antihypertensive, cardioprotective and anticancer (Borlinghaus et al., 2014); the latter being the focus of this study. The mechanisms underpinning the anticancer activity of allicin have been studied (Borlinghaus et al., 2014; Miron et al., 2008), and allicin has been observed to exhibit anticancer activity towards colon cancer (Bat-Chen et al., 2010), gastric cancer SGC-7901 cells (Sun et al., 2014), glioma cells (Li et al., 2018), human cervical cancer SiHa cells (Oommen., 2004), human epithelial carcinoma (Park et al., 2005), liver cancer (Chu et al., 2013), MCF-7 cells (Hirsch et al., 2000), neuroblastoma (Zhuang et al., 2016), ovarian cancer (Xu et al., 2014), and pancreatic cancer (Wang et al., 2013).

Here we report the development of dual stimuli-responsive nanoparticles based on the conjugated polymer PPY. The PPY nanoparticles were loaded with allicin and their ability to deliver allicin in response to the application of an electric field is demonstrated *in vitro*, and to exhibit photothermal toxicity towards HEP G2 cells in response to exposure to irradiation with near infrared light is demonstrated *in vitro*.

2. Materials and Methods

2.1. Materials

Pyrrole, dimethyl sulfoxide (DMSO), phosphate buffered saline tablets (when dissolved in 200 ml deionized water yields 0.01 M PBS, pH 7.4 at $25^{o}C$) and MTT were purchased from Sigma, St. Louis, Mo., USA. Allicin was purchased from Jiangsu Chiatai Qingjiang Pharmaceutical Co., Ltd., China. Spectra/Por® dialysis membrane, 12,000–14,000 molecular weight cut off, was purchased from Spectrum Laboratories Inc., Rancho Dominguez, Canada. Pure platinum electrodes were fabricated by Damas, Cairo, Egypt.

2.2. Methods:

2.2.1. Electropolymerization of allicin-loaded PPY.

An electrochemical polymerization cell was constructed as demonstrated in **Figure S1**. 22.3 mg of allicin and 0.63 ml of pyrrole were dissolved in 10 ml of deionized water. Two pure platinum electrodes were dipped in the solution as shown in **Figure S1** and the setup was covered with in parafilm. The electrodes were connected with electrical wires to the poles of a 9V battery (Philips, Amsterdam, The Netherlands). The electropolymerization process was carried out for 6 hours to ensure the complete formation and deposition of the allicin-doped PPY at the anode.

2.2.2. Determination of the drug content of the PPY films.

The extent of drug loading was performed using an indirect assay method, where the working electrode (the film-deposited platinum electrode) was connected to the negative pole of the used battery and the counter electrode was connected to the positive counterpart. Both electrodes were dipped in a 10 ml of deionized water for 6 hours. An aliquot of 1 ml of the aqueous medium was obtained, filtered using 0.45 µm pore filter (Merck, Burlington, MA) and analyzed using UV spectrophotometry (Shimadzu, Kyoto, Japan) at 212 nm. 11 mg polypyrrole nanoparticles contained 2.2 mg of allicin.

2.2.3. Formation of the allicin-loaded PPY nanoparticles.

Drug-loaded PPY films were scratched off the platinum electrode (the anode) into a test tube containing an aqueous solution of 0.1% (v/v) Tween 80. Probe sonication (Hielscher Ultrasonics GmbH, Teltow, Germany) at 30 kHz and 100% amplitude was conducted for 2 minutes to obtain a homogenous dispersion. The strong electrostatic bonds formed between the PPY matrix and allicin retained the drug in the PPY matrix during the sonication process, as confirmed by the negligible absorbance measurement of the drug content in the supernatant after centrifugation of the dispersion at 15,000 rpm using UV spectrophotometry at 212 nm.

2.2.4. Characterization of the prepared allicin-loaded PPY nanoparticles.

2.2.4.1. Particle size and polydispersity index measurements

The mean particle diameter and polydispersity index (PDI) were determined by dynamic light scattering using a Nano ZS® zetasizer (Zetasizer Nano ZS®, Malvern instruments, Malvern, UK). The sample was diluted with deionized water until weak opalescence was observed. The sample was analyzed using disposable polystyrene cells where the measurements were intensity-based and performed at 25°C with an angle detection of 173°. Particle size was calculated according to the Brownian movement of the nanoparticles utilizing the Stokes–Einstein equation. The measurements were done in triplicate and the means and standard deviations were calculated.

2.2.4.2. Zeta potential measurements

The surface charge of the nanoparticles was determined by measuring the zeta potential. The samples were diluted with 5mM phosphate buffer (pH 7.4) and 1 ml was placed in folded capillary zeta cells. The zeta potential was calculated according to laser Doppler velocimetry using a Nano ZS® zetasizer. The measurements were done in triplicate at 25°C and the means and standard deviations were calculated.

2.2.4.3. Determination of the morphology of the allicin-loaded PPY nanoparticles using transmission electron microscope (TEM)

The shape and morphology of the prepared nanoparticles were examined using a transmission electron microscope (TEM) (Jeol Electron Microscope, JEM-1010, Tokyo, Japan). The samples were diluted (1:40 v/v) with deionized water prior to examination. Then, a droplet of the diluted dispersion was placed on a carbon film-covered copper grid (200-mesh). After five minutes, a filter paper placed at the edge of the copper grid was used to remove any excess liquid present. Samples were air-dried before observation by TEM. The

samples were examined at 120 and 200 kV at a magnification of X50000. No staining was required.

2.2.5. Confirmation of allicin stability in the prepared nanoparticles using ^{1}H-NMR.

The successful loading of allicin in the nanoparticles after sonication was proven by ^{1}H-NMR using a 400 MHz NMR spectrometer (Bruker Avance III, Billerica, MA) after dispersing the nanoparticles in DMSO at 40°C.

2.2.6. Electrically controlled drug release.

The release experiment was carried out by placing the nanoparticles in dialysis bags (10,000-12,000 Daltons) immersed in 10 ml of 0.01 M PBS (pH 7.4). The electrical stimulus for drug release from the prepared nanoparticles was the voltage application of −9 V for 5s followed by 5s of 0 V (for PPY recovery). Such stimulus was found to be most efficient in driving the drug out while minimizing the electrochemical damage to the PPY matrix (Luo et al., 2009). Samples were taken at specified time intervals, replaced by fresh buffer portions and analyzed for allicin content using UV spectrophotometry at 212 nm. The results were compared to the release of the drug from the loaded PPY nanoparticles using the same experimental setup in the absence of the electrical trigger.

2.2.7. Determination of the cytotoxicity and the phototoxicity of the allicin-loaded PPY nanoparticles.

2.2.7.1. Cell culture

Human liver carcinoma HepG2 cell line was obtained from the holding company for biological products and vaccines VACSERA (Giza, Egypt). Cells were maintained at 37°C under a humidified 5% CO_2 atmosphere in RPMI medium containing 10% FBS and 1% penicillin-streptomycin antibiotic mixture (100 IU penicillin and 100 µg streptomycin) (Theriault et al., 1999).

2.2.7.2. Cell viability test

The viability of HepG2 cells in the presence of allicin and allicin-PPY nanoparticles complex (Allicin-PPY) was evaluated by performing MTT (3-(4,5-dimethylthiazol-2-yl)-2,5-diphenyl tetrazolium bromide) assay (Farid et al., 2014; Metwally et al., 2016). HepG2 cells were seeded into 96-well culture plates (~7000 cells/well) containing Roswell Park Memorial Institute medium (RPMI) and 10% fetal bovine serum (FBS), allowed to adhere, and maintained at 37°C for 24 hrs. Then, the media were replaced with the test and control media. Test media were prepared by adding the intended volume of the test samples (aqueous solutions) in RPMI media containing fetal bovine serum in a concentration that reaches 2% upon addition (final FBS concentration is 2%). Control media (specific control for each test) were prepared in the same way as the test media but the added test samples were replaced by the same volume of the plain solvent (i.e. sterilized distilled water). Two concentrations of allicin (50 µg/ml and 100 µg/ml) as well as the corresponding concentrations of allicin-PPY nanoparticles (50/250 µg/ml and 100/500 µg/ml, respectively) were examined simultaneously with their controls (4 wells for each test and control medium). The plates were incubated at 37°C under 5% CO_2 atmosphere. After 48 h, test and control media were replaced by phenol red-free (colorless) RPMI media containing 0.05% MTT (100 µL for each well) and incubated at 37°C for 3–4 h. At the end of the incubation period, MTT media were removed and the purple formazan crystals formed were solubilized by adding dimethyl sulphoxide (DMSO) (200 µL). The concentration of formazan in each culture well was measured from its absorbance at 570 nm using ELISA microplate reader Biotek *Elx800*, USA. Being directly proportional to formazan concentration, viability was calculated by dividing the mean readings of test media-treated wells by those of their specific controls (in percentage). To evaluate photocytotoxicity, identical experiments were performed after 48 h., and before the MTT step, test and control media were replaced by phenol red-free RPMI media (100 µL per well) and the plates were then irradiated under white light of a halogen lamp (OSHINO lamps

GMBH, Nurnberg, Germany) (covering a wide range of wavelengths in the UV and NIR regions, 1W) for 30 minutes. After irradiation, media were replaced with RPMI media containing 10% FBS and incubated at 37°C under 5% CO_2 atmosphere for 24 h., then MTT step was applied as mentioned above. All cytotoxicity and photocytotoxicity experiments were carried out under the same conditions. Experiments were repeated at least three times and means and standard deviations are reported.

3. Results and Discussion

3.1. Preparation and characterization of allicin-loaded PPY nanoparticles.

Drug-loaded PPY nanoparticles were successfully prepared using electropolymerization. Allicin (**Figure 1B**) is negatively charged and can dope positively charged PPY (Durlak et al., 2016), and the nanoparticles produced had a negative zetapotential of -9.77 ± 1.3 mV which may be beneficial for the colloidal stability of the nanoparticles due to charge-charge repulsion (Mehanny et al., 2016). Transmission electron microscopy (TEM) imaging of the nanoparticles and revealed their pseudo-spherical morphology. The particles sizes of the nanoparticles determined by TEM (ca. 40-180 nm, **Figure 2A** and **2B**) were smaller than those determined by dynamic laser scattering (DLS) which estimated particle sizes to be 275 ± 34 nm and a low PDI of 0.216 ± 0.1 (**Figure 2C**). This disparity in size is because TEM imaging relies upon dry/dehydrated particles on a hydrophobic carbon-coated grid (which can yield a lower volume nanoparticles and even enhance the particles aggregation as shown in **Figure 2B**) (Lao et al., 2010); and DLS measurements are carried out on hydrated samples and it is an intensity-based particle size measurement technique which relies on Raleigh's equation in which the intensity of scattered light is proportional to the diameter of particles and consequently biased to larger particles (Stetfeld et al., 2016).

The loading of allicin in the PPY matrix was confirmed by ^{1}H-NMR analysis, where the characteristic peaks of allicin at 3.5-4 ppm and 4.5-5.5 ppm corresponding to the –CH$_2$ groups located next to the sulphur atoms and the hydrogens of the -CH=CH- groups, respectively were clearly visible in the ^{1}H-NMR spectra of the allicin loaded-nanoparticles (**Figure S2**) (Lu et al., 2014; Soumya et al., 2018).

3.2. Electrochemically-triggered delivery of allicin.

Electroactive drug delivery devices where the delivery of the therapeutic can be controlled in an on/off fashion are particularly interesting as they have the potential to control the chonopharmacology of the drug in line with the chronobiology of the condition to be treated. A variety of drugs have been delivered from PPY matrices when exposed to electrical fields which encourage migration of ions into and out of the polymer matrix (Ateh et al., 2006). Control electrochemical release experiments (described in section 2.2.2.) show that 11 mg polypyrrole nanoparticles contained 2.2 mg of allicin. Over the period of an hour ca. 25% of the allicin load was released from the nanoparticles by passive leaching of the drug from the matrix, whereas, when exposed to an electrical field all of the allicin was released from the allicin-loaded PPY nanoparticles (**Figure 3**). These results demonstrate the potential of the nanoparticles to deliver a therapeutically relevant dose of allicin, particularly if the nanoparticles were locally delivered to tissues.

3.3. Cytotoxicity and photocytotoxicity of the allicin-loaded PPY nanoparticles.

Allicin and allicin-PPY nanoparticles (50 µg/ml, 100 µg/ml and 50/250 µg/ml, 100/500 µg/ml, respectively) had no significant effect (p < 0.05) on HepG2 cells under dark conditions. Free allicin resulted in slight reductions in cell viability when increasing its concentration under the applied irradiation conditions. In contrast, irradiation of allicin-PPY treated cells (50/250 µg/ml and 100/500 µg/ml) under the same irradiation conditions led to significant decreases in cell viability (p > 0.05) by about 20 % and 30 %, respectively

(**Figure 4**). This decrease in cell viability could be attributed to the photothermal activity of PPY nanoparticles (Wang et al., 2015; Wang et al., 2016). Visible-NIR light spectroscopy showed allicin-loaded PPY nanoparticles absorb light in the NIR region (**Figure S3**). Since there is a wide IR band in the white light spectrum, a photothermal action is exerted by the PPY nanoparticles leading to hyperthermia of the cells which results in cell death (Liu et al., 2016). Therefore, allicin-loaded PPY nanoparticles can be used at a relatively high concentration (up to 500 µg/ml) with photothermal activity under conventional white light.

4. Conclusion

The dual stimuli-responsive nanoparticles for anticancer therapy reported here represent an interesting potential platform for the treatment of cancer and a variety of other conditions. It would be possible to harness the utility of the photothermal effect of the PPY nanoparticles on other cells displaying undesirable behavior to treat a variety of medical conditions. Although allicin was used as a model anticancer drug (primarily because it is straightforward to quantify its release using UV-vis spectroscopy), it is noteworthy that a wide variety of other bioactive molecules could be loaded into the polymer nanoparticles using the same experimental paradigm. We foresee the potential of the nanoparticles described herein to treat a variety of conditions, and moreover, biodegradable versions of such nanoparticles (Hardy et al, 2014; Hardy et al., 2015).

Declaration of Interest

The authors report no conflicts of interest.

Figure Captions:

Figure 1. Structures of the components of the drug delivery system. A) PPY. B) Allicin.

Figure 2. Size determination of the nanoparticles. A and B) TEM images of the allicin-loaded PPY nanoparticles. C) DLS data of particle size distribution and polydispersity index of the allicin-loaded PPY nanoparticles.

Figure 3. *In vitro* validation of the electrochemically-triggered release of allicin from allicin-loaded PPY nanoparticles.

Figure 4. *In vitro* validation of the photothermal toxicity of the PPY nanoparticles. Assessment of the cytotoxicity of allicin and allicin-loaded PPY (Allicin-PPYNP) nanoparticles towards HepG2 cells in the absence or presence of light.

References

Abozeid, S.M., Hathout, R.M., Abou-Aisha, K., 2016. Silencing of the metastasis-linked gene, AEG-1, using siRNA-loaded cholamine surface-modified gelatin nanoparticles in the breast carcinoma cell line MCF-7. Colloids Surf. B Biointerfaces, 145, 607-616.

Ateh, D.D., Navsaria, H.A., Vadgama, P., 2006. Polypyrrole-based conducting polymers and interactions with biological tissues. J R. Soc. Interface, 3, 741-752.

Balint, R., Cassidy, N.J., Cartmell, S.H., 2014. Conductive polymers: towards a smart biomaterial for tissue engineering. Acta Biomater., 10, 2341-2353.

Bat-Chen, W., Golan, T., Peri, I., Ludmer, Z., Schwartz, B., 2010. Allicin purified from fresh garlic cloves induces apoptosis in colon cancer cells via Nrf2. Nutr. Cancer, 62, 947-957.

Borden, E.C., Esserman, L., Linder, D.J., Campbell, M.J., Fulton, A.M., 1999. Biological therapies for breast carcinoma: concepts for improvement in survival. Semin. Oncol., 26, 28-40.

Borlinghaus, J., Albrecht, F., Gruhlke, M.C., Nwachukwu, I.D., Slusarenko, A.J., 2014. Allicin: chemistry and biological properties. Molecules, 19, 12591-12618.

Chen, G., Ma, B., Xie, R., Wang, Y., Dou, K., Gong, S., 2017. NIR-induced spatiotemporally controlled gene silencing by upconversion nanoparticle-based siRNA nanocarrier. J Control Release. doi: 10.1016/j.jconrel.2017.12.028

Chu, Y.L., Ho, C.T., Chung, J.G., Raghu, R., Lo, Y.C., Sheen, L.Y., 2013. Allicin induces anti-human liver cancer cells through the p53 gene modulating apoptosis and autophagy. J Agric. Food Chem., 61, 9839-9848.

Curt, G.A., 1996. Cancer Drug Development: New Targets for Cancer Treatment. Oncologist., 1, II-III.

Durlak, P., Berski, S., Latajka, Z., 2016. Theoretical studies on the molecular structure, conformational preferences, topological and vibrational analysis of allicin. Chemical Physics Letters, 644, 5-13.

Farid, M.M., Hathout, R.M., Fawzy, M., bou-Aisha, K., 2014. Silencing of the scavenger receptor (Class B - Type 1) gene using siRNA-loaded chitosan nanaoparticles in a HepG2 cell model. Colloids Surf. B Biointerfaces, 123, 930-937.

Fonner, J.M., Forciniti, L., Nguyen, H., Byrne, J.D., Kou, Y.F., Syeda-Nawaz, J., Schmidt, C.E., 2008. Biocompatibility implications of polypyrrole synthesis techniques. Biomed. Mater., 3, 034124.

Hardy, J.G., Mouser, D.J., Arroyo-Currás, N., Geissler, S., Chow, J.K., Nguy, L., Kim, J.M., Schmidt, C.E., 2014, Biodegradable electroactive polymers for electrochemically-triggered drug delivery. J. Mater. Chem. B, 2(39), 6809-6822. DOI: 10.1039/C4TB00355A.
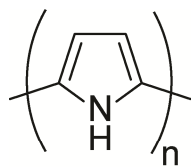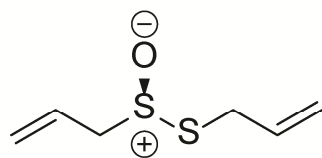
Hardy, J.G., Amend, M.N., Geissler, S., Lynch, V.M., Schmidt, C.E., 2015, Peptide-directed assembly of functional supramolecular polymers for biomedical applications: electroactive molecular tongue-twisters (oligoalanine-oligoaniline-oligoalanine) for electrochemically enhanced drug delivery. J. Mater. Chem. B, 3(25), 5005-5009. DOI: 10.1039/C5TB00106D.

Hirsch,K., Danilenko, M., Giat, J., Miron, T., Rabinkov, A., Wilchek, M., Mirelman, D., Levy, J., Sharoni, Y., 2000. Effect of purified allicin, the major ingredient of freshly crushed garlic, on cancer cell proliferation. Nutr. Cancer, 38, 245-254.

Lao, S.B., Zhang, Z.X., Xu, H.H., Jiang, G.B., 2010. Novel amphiphilic chitosan derivatives: Synthesis, characterization and micellar solubilization of rotenone. Carbohydrate Polymers, 82, 1136-1142.

Li, C., Jing, H., Ma, G., Liang, P., 2018. Allicin induces apoptosis through activation of both intrinsic and extrinsic pathways in glioma cells. Mol Med. Rep., 17, 5976-5981.

Liu, M., Xu, N., Liu, W., Xie, Z., 2016. Polypyrrole coated PLGA core-shell nanoparticles for drug delivery and photothermal therapy. RSC Adv., 6, 84269-84275.

Lu, Q., Lu, P.M., Piao, J.H., Xu, X.L., Chen, J., Zhu, L., Jiang, J.G., 2014. Preparation and physicochemical characteristics of an allicin nanoliposome and its release behavior. LWT - Food Science and Technology, 57, 686-695.

Luo, X., Cui, X.T., 2009. Sponge-like nanostructured conducting polymers for electrically controlled drug release. Electrochem. Commun., 11, 1956.

Mehanny, M., Hathout, R.M., Geneidi, A.S., Mansour, S., 2016. Bisdemethoxycurcumin loaded polymeric mixed micelles as potential anti-cancer remedy: Preparation, optimization and cytotoxic evaluation in a HepG-2 cell model. Journal of Molecular Liquids, 214, 162-170.

Metwally, A.A., El-Ahmady, S.H., Hathout, R.M., 2016. Selecting optimum protein nano-carriers for natural polyphenols using chemoinformatics tools. Phytomedicine., 23, 1764-1770.

Miron, T., Wilchek, M., Sharp, A., Nakagawa, Y., Naoi, M., Nozawa, Y., Akao, Y., 2008. Allicin inhibits cell growth and induces apoptosis through the mitochondrial pathway in HL60 and U937 cells. J. Nutr. Biochem., 19, 524-535.

Oommen, S., Anto, R.J., Srinivas, G., Karunagaran, D., 2004. Allicin (from garlic) induces caspase-mediated apoptosis in cancer cells. Eur. J Pharmacol., 485, 97-103.

Park, S.Y., Cho, S.J., Kwon, H.C., Lee, K.R., Rhee, D.K., Pyo, S., 2005. Caspase-independent cell death by allicin in human epithelial carcinoma cells: involvement of PKA. Cancer Lett., 224, 123-132.

Pillay,V., Tsai,T.S., Choonara,Y.E., du Toit,L.C., Kumar,P., Modi,G., Naidoo,D., Tomar, L.K., Tyagi, C., Ndesendo, V.M., 2014. A review of integrating electroactive polymers as responsive systems for specialized drug delivery applications. J. Biomed. Mater. Res. A, 102, 2039-2054.

Song, X., Liang, C., Feng, L., Yang, K., Liu, Z., 2017. Iodine-131-labeled, transferrin-capped polypyrrole nanoparticles for tumor-targeted synergistic photothermal-radioisotope therapy. Biomater. Sci, 5, 1828-1835.

Soumya, R.S., Sherin, S., Raghu, K.G., Abraham, A., 2018. Allicin functionalized locust bean gum nanoparticles for improved therapeutic efficacy: An in silico, in vitro and in vivo approach. Int. J. Biol. Macromol., 109, 740-747.

Stetefeld, J., McKenna, S.A., Patel, T.R., 2016. Dynamic light scattering: a practical guide and applications in biomedical sciences. Biophys. Rev., 8, 409-427.

Sun, L., Wang, X., 2003. Effects of allicin on both telomerase activity and apoptosis in gastric cancer SGC-7901 cells. World J. Gastroenterol., 9, 1930-1934.
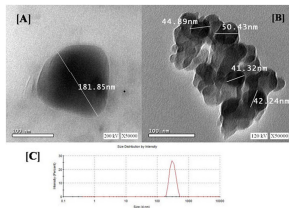
Theriault, A., Wang, Q., Gapor, A., Adeli, K., 1999. Effects of gamma-tocotrienol on ApoB synthesis, degradation, and secretion in HepG2 cells. Arterioscler. Thromb. Vasc. Biol, 19, 704-712.

Tibbitt, M.W., Rodell, C.B., Burdick, J.A., Anseth, K.S., 2015. Progress in material design for biomedical applications. Proc Natl Acad Sci USA, 112, 14444.

Uppalapati, D., Boyd,B. J., Garg, S., Travas-Sejdic, J., Svirskis, D., 2016. Conducting polymers with defined micro- or nanostructures for drug delivery. Biomaterials, 111, 149-162.

Wang, C. J., Wang, C., Han, J., Wang, Y.K., Tang, L., Shen, D.W., Zhao, Y., Xu, R.H., Zhang, H., 2013. Effect of combined treatment with recombinant interleukin-2 and allicin on pancreatic cancer. Mol. Biol. Rep., 40, 6579-6585.

Wang, J., Lin, F., Chen, J., Wang, M., Ge, X., 2015. The preparation, drug loading and in vitro NIR photothermal-controlled release behavior of raspberry-like hollow polypyrrole microspheres. J. Mater. Chem. B, 3, 9186-9193.

Wang, J., Rong, J., Fang, Z., Wang, M., Asif, A., Wu, Q., Zhou, X., Ge, X., 2017. Monodisperse Polypyrrole Nanoparticles Prepared via gamma-Ray Radiolysis of Water: An Efficient Near-Infrared Photothermal Agent for Cancer Therapy. Part. Part. Syst. Charact., 34, 1600430-1600n/a.

Wang, M., 2016. Emerging Multifunctional NIR Photothermal Therapy Systems Based on Polypyrrole Nanoparticles. Polymers, 8(10), 373.

Xu, L., Yu, J., Zhai, D., Zhang, D., Shen, W., Bai, L., Cai, Z., Yu, C., 2014. Role of JNK Activation and Mitochondrial Bax Translocation in Allicin-Induced Apoptosis in Human Ovarian Cancer SKOV3 Cells. Evid. Based. Complement Alternat. Med., 2014, 378684.

Zhuang, J., Li, Y., Chi, Y., 2016. Role of p38 MAPK activation and mitochondrial cytochrome-c release in allicin-induced apoptosis in SK-N-SH cells. Anticancer Drugs, 27, 312-317.
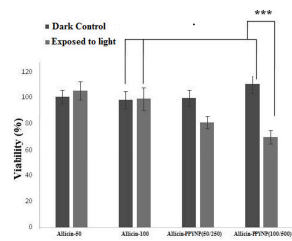
A

B